References and Notes

(1) N. G. McCrum, B. E. Read, and G. Williams, "Anelastic and Dielectric Effects in Polymeric Solids", Wiley, New York, N.Y., 1967.
(2) H. E. Bommel and K. Dransfeld, *Phys. Rev.*, **117**, 1245 (1960).
(3) A. B. Bhatia, "Ultrasonic Absorption", Clevendon Press, Oxford, 1967.
(4) A. M. North and R. A. Pethrick, "Transfer and Storage of Energy by Molecules", Vol. 4, G. M. Burnett, A. M. North, and J. N. Sherwood, Ed., Wiley, London, 1974.
(5) C. Zener, *Proc. Phys. Soc., London*, **52**, 152 (1940).
(6) T. Wright and D. D. Campbell, in press.
(7) K. G. Plass, *Acustica*, **19**, 236 (1968).
(8) V. F. Nozdrev, "The Use of Ultrasonics in Molecular Physics", Pergammon Press, Oxford, 1965.
(9) E. L. Heasell and J. Lamb, *Proc. Phys. Soc., London, Sect. B*, **69**, 869 (1956).
(10) M. Francon, "Optical Interferometry", Academic Press, New York, N.Y., 1966.
(11) J. B. Jackson, P. J. Flory, and R. Chiang, *Trans. Faraday Soc.*, **59**, 1906 (1963).
(12) H. A. Waterman, *Kolloid-Z.*, **192**, 1 (1963).
(13) R. F. Boyer, *J. Polym. Sci., Polym. Symp.*, **50**, 189 (1975).
(14) A. Tanaka, E. P. Chang, B. Delf, I. Kimura, and R. S. Stein, *J. Polym. Sci., Polym. Phys. Ed.*, **11**, 1891 (1973).
(15) Z. H. Stachurski and I. M. Ward, *J. Macromol. Sci., Phys.*, **3**, 445 (1969).
(16) J. B. Smith, G. R. Davies, G. Cappaccio, and I. M. Ward, *J. Polym. Sci., Polym. Phys. Ed.*, **13**, 2331 (1975).
(17) W. G. Oakes and D. W. Robinson, *J. Polym. Sci.*, **14**, 505 (1954).
(18) R. W. Gray and N. G. McCrum, *J. Polym. Sci., Part A-2*, **7**, 1329 (1969).
(19) H. A. Flocke, *Kolloid-Z.*, **180**, 118 (1962).
(20) N. G. McCrum, *J. Polym. Sci., Polym. Lett. Ed.*, **2**, 495 (1964).
(21) A. J. Owen and I. M. Ward, *J. Macromol. Sci., Phys.* **7**, 417 (1973).
(22) D. C. Douglass, D. R. Falcone, and V. J. McBrierty, *J. Chem. Soc., Faraday Trans. 2*, **68**, 1051 (1972).
(23) A. J. Curtis, *Prog. Dielectr.*, **2**, 31 (1960).
(24) W. Sommer, *Kolloid-Z.*, **167**, 97 (1959).
(25) G. Pezzin, G. Ajroldi, T. Casiraghi, C. Garbugho, and G. Vittadim, *J. Appl. Polym. Sci.*, **16**, 1839 (1972).
(26) Y. Ishida, *Kolloid-Z.*, **168**, 29 (1960).
(27) J. A. Manson, S. A. Iobst, and R. Acosta. *J. Macromel. Sci., Phys.*, **9**, 301 (1974).
(28) D. A. Jackson, H. T. A. Pentecost, and J. G. Powles, *Mol. Phys.*, **23**, 425 (1972).
(29) E. P. Papadakis, *J. Appl. Phys.*, **34**, 265 (1963).
(30) K. Neki and P. H. Geil, *J. Macromol. Sci., Phys.* **8**, 295 (1973).
(31) R. G. Quynn, J. L. Riley, D. A. Young, and H. D. Noether *J. Appl. Polym. Sci.*, **2**, 166 (1959).
(32) Y. Maeda, *J. Polym. Sci.*, **18**, 87 (1955).
(33) T. Alfrey, Jr., N. Wiederhorn, R. Stein, and A. V. Tobolsky, *J. Colloid Sci.*, **4**, 211 (1949).
(34) A. Akheiser, *J. Phys. (Moscow)*, **1**, 277 (1939).
(35) K. Brugger, *Phys. Rev.*, **133**, A1611 (1964).
(36) H. E. Bommel and K. Dransfeld, *Phys. Rev.*, **117**, 1245 (1960).
(37) T. O. Woodruff and E. Ehrenreich, *Phys. Rev.*, **123**, 1553 (1961).
(38) G. S. Cieloszyk, M. T. Cruz, and G. L. Salinger, *Cryogenics*, **13**, 718 (1973).
(39) H. J. Maris, "Physical Acoustics", Vol. VII, W. P. Mason and R. N. Thurston, Ed., Academic Press, New York, N.Y., 1971.
(40) G. Liebfried, *Z. Phys.*, **127**, 344 (1950).
(41) W. P. Mason, *J. Acoust. Soc. Am.*, **32**, 458 (1960).
(42) S. Takahaski, *J. Phys. Soc. Jpn.*, **11**, 1253 (1956).
(43) P. G. Bordoni, *J. Acoust. Soc. Am.*, **26**, 495 (1954).
(44) T. S. Hutchison and D. H. Rogers, *J. Appl. Phys.*, **33**, 792 (1962).
(45) L. J. Bruner, *Phys. Rev.*, **118**, 399 (1960).
(46) E. M. Lifschitz and G. D. Parkhomovskii, *Zh. Eksp. Teor. Fiz.*, **20**, 175 (1950).
(47) H. B. Huntington, *J. Acoust. Soc. Am.*, **22**, 362 (1950).
(48) A. B. Bhatia and R. A. Moore, *J. Acoust. Soc. Am.*, **31**, 1140 (1959).
(49) R. Truell, C. Elbaum, and B. B. Chick, "Ultrasonic Methods in Solid State Physics", Academic Press, New York, N.Y., 1969.
(50) J. R. Dillinger, D. L. Fehl, and R. P. Madding, *J. Polym. Sci., Polym. Phys. Ed.*, **11**, 1435 (1973).
(51) B. Hartmann and J. J. Arzynski, *J. Acoust. Soc. Am.*, **56**, 1469 (1974).
(52) D. E. Kline, *J. Polym. Sci.*, **50**, 441 (1961).
(53) A. D. Pasguino and M. N. Pitsworth, *J. Polym. Sci., Part B*, **2**, 253 (1964).
(54) B. Wunderlich and H. Baur, *Adv. Polym. Sci.*, **7**, 151 (1970).
(55) C. Zener, *Proc. Phy. Soc., London*, **52**, 152 (1940).
(56) C. Zener, "Elasticity and Anelasticity of Metals", Chicago University Press, Chicago, Ill., 1948.
(57) D. W. Van Krevelen, "Properties of Polymers: Correlations with Chemical Structure", Elsevier, Amsterdam, 1972.
(58) R. C. Weast, Ed., "Handbook of Chemistry and Physics", 55th ed., Chemical Rubber Publishing Co., Cleveland, Ohio, 1974–75.

Crystal Structures of Optically Active and Inactive Poly(*tert*-butylethylene sulfide)

Hajime Matsubayashi,[1a] Yozo Chatani,[1a] Hiroyuki Tadokoro,*[1a] Philippe Dumas,[1b] Nicolas Spassky,[1b] and Pierre Sigwalt[1b]

Department of Polymer Science, Faculty of Science, Osaka University, Toyonaka, Osaka 560, Japan, and Laboratoire de Chimie Macromoléculaire associé au C.N.R.S. Université de Paris VI, Paris 5e, France.

Received May 4, 1977

ABSTRACT: The molecular and crystal structures of optically active and inactive poly(*tert*-butylethylene sulfide) were determined by x-ray analysis. Crystals of the optically active species are trigonal, $P3_1$-C_3^2, with cell dimensions a = 16.91 Å and c(fiber axis) = 6.50 Å. Three isotactic right-handed (3/1) helical chains possessing essentially $(SG\bar{S})_3$ conformation for the sinister configuration pass through the unit cell. The reflection intensities are, however, explained in terms of a statistical molecular packing with respect to upward and downward chains. Crystals of the optically inactive species are monoclinic, $P2_1/a$-C_{2h}^5, and the cell dimensions are a = 16.67 Å, b = 19.27 Å, c(fiber axis) = 6.52 Å, and β = 90°. The main chain conformation is essentially the same as that of the active species. Two pairs of rectus and sinsiter molecular chains pass through the unit cell; the optical compensation of the racemic polymer is attained by the formation of the racemic lattice. Remarkable difference in melting point and solubility for both the species might be explained in terms of these crystal structures.

In previous papers, we reported the crystal structures of several isotactic polymers which have true asymmetric carbon atoms in the main chain: poly(*tert*-butylethylene oxide),[2] poly(propylene sulfide),[3] poly(β-hydroxy butyrate),[4] poly(β-ethyl-β-propiolactone),[5] and poly(isopropylethylene oxide).[6] In these polymers, there are two kinds of optical isomers. According to the nomenclature proposed by Cahn, Ingold, and Prelog,[7] the absolute configurations of these two optical isomers can be indicated by rectus and sinister. Three modes of optical compensation in these racemic species were proposed.[2,3] In the case of the optically inactive poly(*tert*-butylethylene oxide), three crystalline forms are observed depending on the crystallization conditions. One of them forms a racemic lattice, the unit cell of which contains two pairs of rectus and sinister molecular chains. On the contrary, the crystallite of the second form contains only rectus (or sinister) chains; the optical compensation in this case is attained by the presence of equal amounts of crystallites of

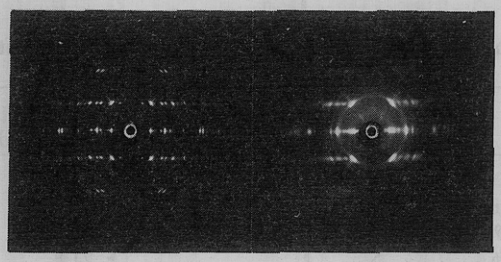

(a) (b)

Figure 1. X-ray fiber photographs of poly(*tert*-butylethylene sulfide): (a) optically active species; (b) optically inactive species.

rectus and of sinister chains (intercrystallite compensation). In all the other polymers mentioned above, the modes of optical compensation in the inactive species are thus of an intercrystallite nature. In the present study, crystal structures were determined for the optically active and inactive poly(*tert*-butylethylene sulfide) polymerized using diethylzinc–water (1:1) as the catalyst. We demonstrate that both the optically active and inactive species are composed of isotactic chains possessing the same main chain conformation, but with differing crystal structures.

Experimental Section

Samples. Optically active and inactive poly(*tert*-butylethylene sulfide) used in this study were synthesized by the method in ref 8 and 9. The optically active polymer was prepared from (*S*)-*tert*-butylethylene sulfide using diethylzinc–water as the catalyst. The optical rotation of the monomer is $\alpha_m = -35°$ (neat, dm), and that of the resulting polymer is $[\alpha]^{25}_D = 172°$ ($CHCl_3$). The optically inactive polymer was prepared in an analogous manner from racemic *tert*-butylethylene sulfide. The melting point measured by using a polarizing microscope was about 210 °C for the optically inactive polymer and about 162 °C for the optically active polymer. Uniaxially oriented specimens were prepared by stretching at 70 °C in water after melting and subsequent quenching in dry ice–methanol. The optically active specimens were annealed at 145 °C for 30 h. A uniaxially oriented specimen of the inactive species of sufficient crystallinity for x-ray analysis was obtained by annealing a stretched specimen in Wood's alloy at 185 °C for 5 h.

X-Ray Diffraction. X-ray fiber photographs were taken with nickel-filtered Cu Kα radiation. The fiber photographs of the optically active and inactive species are shown in Figures 1a and 1b, respectively. In particular, the Bragg angles, measured by the use of a cylindrical camera of radius 100 mm, were calibrated with reference to those of aluminum powder. The reflection intensities obtained by the multiple-film method were estimated by visual comparison with a standard intensity scale. The intensities were corrected for the single-crystal rotation Lorentz–polarization factor. In addition, Weissenberg photographs were taken by setting the uniaxially oriented specimen with the fiber axis perpendicular to the camera axis in order to measure meridional reflections.

Structure Analysis

Unit Cell and Space Group. A total of 88 independent Bragg reflections were observed for the inactive species and 79 for active species. Crystal data are listed in Table I. The densities were measured by the flotation method in $CaCl_2$ aqueous solution. Crystals of the optically active species are trigonal and nine monomeric units are contained in the unit cell. The fiber period is 6.50 Å. Therefore, it is reasonable to assume that three (3/1) helical chains possessing isotactic configuration pass through the unit cell. The molecular structure of the inactive species is also assumed to be the same based on a fiber period of 6.52 Å and a pseudo-systematic absence ($00l$: $l \neq 3n$) observed on the Weissenberg photograph. The monoclinic space group was adopted for the inactive species, though the crystal axes are orthogonal.

Conformational Analysis. A conformational analysis was performed in order to select the most plausible molecular

Table I
Crystal Data of Poly(*tert*-butylethylene Sulfide)

Optical activity	Active	Inactive
Crystal system	Trigonal	Monoclinic
Space group	$P3_1$-C_3^2	$P2_1/a$-C_{2h}^5
Cell constants		
a, Å	16.91	16.67
b, Å		19.27
c(fiber axis), Å	6.50	6.52
β, deg		90.0
Molecular structure	(3/1) helix	(3/1) helix
No. of helices/ unit cell	3	4
Density, g/cm^3		
X ray	1.08	1.10
Obsd	1.05	1.05

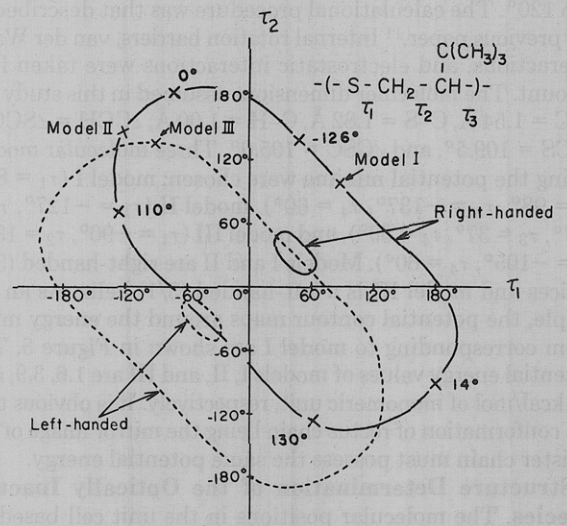

Figure 2. Three-dimensional closed curves representing possible conformations of the main chain of poly(*tert*-butylethylene sulfide).

models. The numbering of the internal rotation angles of the main chain, τ_1, τ_2, and τ_3, and of the side chain, τ_4, is denoted as follows.

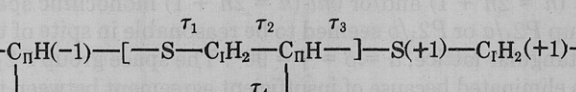

τ_1 [$C_{II}(-1)SC_IC_{II}$], τ_2 [$SC_IC_{II}S(+1)$],

τ_3 [$C_IC_{II}S(+1)C_I(+1)$], and τ_4 [$HC_{II}C_{III}Me$]

The possible conformations of the main chain could be restricted by using the helical parameter equations proposed by Miyazawa,[10] under the assumption of a (3/1) helix with the fiber period of 6.52 Å. The possible sets of the three independent internal rotation angles of the main chain form four closed curves in a cube defined by the three-dimensional Cartesion coordinates, τ_1, τ_2, and τ_3, each covering a range of −180 to 180°. Here we used the convention that trans corresponds to a dihedral angle of 180°. In Figure 2, the projection of these curves on the $\tau_1\tau_2$ plane is shown and only several values of τ_3 are given. The large closed curves represent the (3/1) helices and the small ones (3/2) helices which are derived simultaneously by the use of the helical parameter equations. The closed curves shown by solid lines correspond to right-handed helices and those shown by broken lines to left-handed helices.

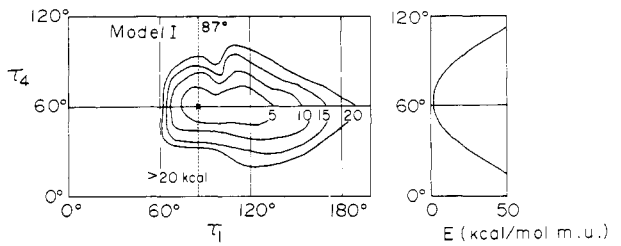

Figure 3. Potential energy map of neighbors of a potential minimum of molecular model I.

The intramolecular potential energies of the sinister configuration were then calculated for the right- and left-handed helical conformations on the four closed curves, in which the internal rotation angle of the side chain, τ_4, was varied from 0 to 120°. The calculational procedure was that described in the previous paper.[11] Internal rotation barriers, van der Waals interactions, and electrostatic interactions were taken into account. The moleculer dimensions assumed in this study are C–C = 1.54 Å, C–S = 1.82 Å, C–H = 1.00 Å, ∠CCH = ∠SCC = ∠CCS = 109.5°, and ∠CSC = 105.0°. Three molecular models giving the potential minima were chosen; model I (τ_1 = 87°, τ_2 = 98°, τ_3 = −137°, τ_4 = 60°), model II (τ_1 = −127°, τ_2 = 147°, τ_3 = 37°, τ_4 = 60°), and model III (τ_1 = −90°, τ_2 = 135°, τ_3 = −105°, τ_4 = 60°). Models I and II are right-handed (3/1) helices and model III is a left-handed (3/1) helix. As an example, the potential contour maps around the energy minimum corresponding to model I are shown in Figure 3. The potential energy values of models I, II, and III are 1.6, 3.9, and 2.0 kcal/mol of monomeric unit, respectively. It is obvious that the conformation of rectus chain being the mirror image of the sinister chain must possess the same potential energy.

Structure Determination of the Optically Inactive Species. The molecular positions in the unit cell based on three molecular models were sought by a trial-and-error method. At first, a comparison between the observed and calculated intensities of the equatorial $hk0$ reflections was examined. From the systematic absences $h00$ ($h = 2n + 1$) and $0k0$ ($k = 2n + 1$) the plane group of the ab plane was determined to be pgg. Models II and III were rejected at this point because of poor agreement between the observed and calculated intensities. Next, from the apparent systematic absences $h0l$ ($h = 2n + 1$) and/or $0kl$ ($k = 2n + 1$) monoclinic space group $P2_1/a$ or $P2_1/b$ seemed to be reasonable in spite of the rectangular lattice, $\alpha = \beta = \gamma = 90°$. The space group $P2_1/b$ was eliminated because of insufficient agreement between the observed and calculated hkl intensities. From the trial-and-error procedure we thus concluded that the space group is $P2_1/a$ and the crystal lattice is composed of molecules described by model I. The constrained least-squares method[12,13] was applied to refine the crystal model. During the refinement, bond lengths and bond angles were fixed as the same values as in the potential energy calculation. The final parameters determined are listed in Table II. The discrepancy factor $R = \Sigma|I_0^{1/2} - I_c^{1/2}|/\Sigma I_0^{1/2}$ was 0.18. The fractional atomic coordinates derived from the final parameters are listed in Table III. Table IV gives the comparison between the observed and calculated spacings and intensities. The crystal structure is shown in Figure 4.

Structure Determination of Active Species. Most of the intense reflections were found to be indexed by a trigonal subcell with cell dimensions, a = 9.76 Å and c(fiber axis) = 6.50 Å. The subcell, which is shown by broken lines in Figure 5, contains only one molecular chain. Therefore, as a first approximation it was assumed that molecular chains were packed at corners of the subcell. The space group of the original cell was reasonably assumed to be $P3_1$ or $P3_2$; the molecular structure is of a right-handed helix in the case of $P3_1$ and is a left-handed helix in $P3_2$. In Figure 5, the assumed molecular packing of the right-handed helices is shown. The molecular packing, based on the three starting models I, II, and III, was sought by a trial-and-error method for the subcell. A disordered structure wherein upward and downward helices of model I are packed in one site with 1:1 ratio was found to be plausible. The molecular packing approximately obeyed

Table II
Final Parameters Obtained by Constrained Least-Squares Refinement of Inactive Polymer[a]

Parameter	Value	Stand dev
Overall temperature factor (Å^2)	8.6	0.9
Eulerian angles, deg		
θ	155.8	3.6
ϕ	71.8	5.4
χ	280.4	4.2
Fractional coordinates of origin atom, S(1)		
x	0.012	0.003
y	0.158	0.003
z	0.351	0.007
Internal rotation angles, deg		
S(1)–C(1)–C(2)–S(2)	60.1	4.2
C(1)–C(2)–S(2)–C(7)	−122.9	2.2
C(2)–S(2)–C(7)–C(8)	115.5	3.4
S(2)–C(7)–C(8)–S(3)	68.4	3.4
C(7)–C(8)–S(3)–C(13)	−126.3	2.6
C(8)–S(3)–C(13)–C(14)	121.2	3.5
S(3)–C(13)–C(14)–C(15)	174.0	3.8
C(13)–C(14)–C(15)–C(17)	178.5	5.6
C(1)–C(2)–C(3)–C(5)	184.4	5.1
C(7)–C(8)–C(9)–C(11)	178.2	5.9

[a] Atoms are numbered as follows

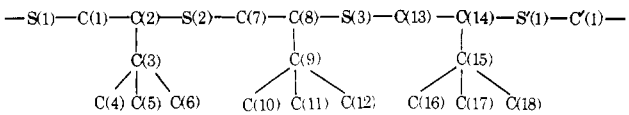

Fixed distances between successive chain units are C(14)–S′(1) = 1.82 Å, C(14)–C′(1) = 2.888 Å, C(13)–S′(1) = 2.748 Å, and C(17)–S′(1) = 2.748 Å.

Table III
Atomic Parameters in Fractional Coordinates of Inactive Polymer[a]

	x	y	z
S(1)	0.012	0.158	0.351
C(1)	0.108	0.114	0.330
C(2)	0.175	0.162	0.414
S(2)	0.155	0.182	0.682
C(7)	0.150	0.277	0.694
C(8)	0.065	0.300	0.754
S(3)	0.045	0.275	1.019
C(13)	−0.047	0.225	1.010
C(14)	−0.033	0.152	1.096
C(15)	−0.113	0.112	1.110
C(17)	−0.098	0.038	1.191
C(3)	0.256	0.125	0.396
C(5)	0.322	0.170	0.495
C(4)	0.252	0.055	0.507
C(6)	0.277	0.113	0.168
C(9)	0.058	0.379	0.733
C(11)	−0.028	0.402	0.787
C(10)	0.017	0.415	0.880
C(12)	0.077	0.400	0.511
C(16)	−0.170	0.151	1.258
C(18)	−0.152	0.108	0.896

[a] Numbers of atoms are the same as Table II.

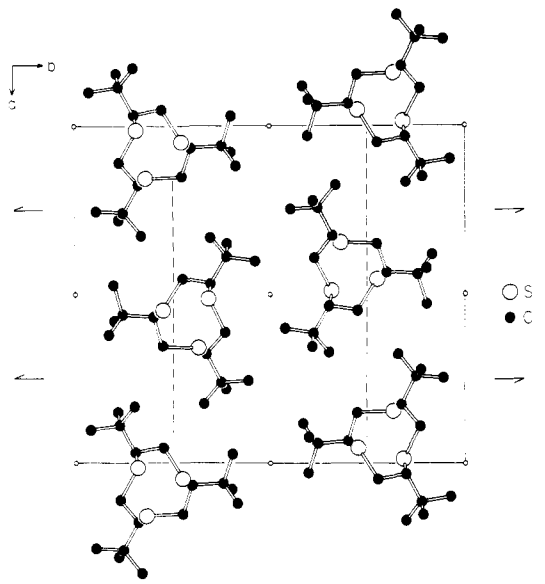

Figure 4. Crystal structure of optically inactive poly(*tert*-butylethylene sulfide).

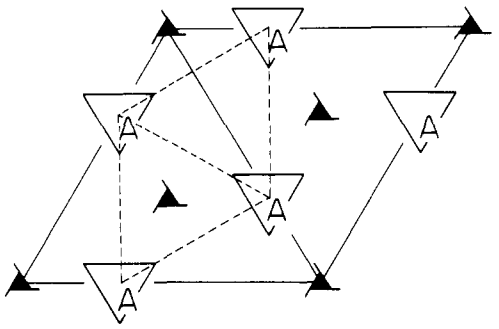

Figure 5. The mode of the molecular packing of optically active poly(*tert*-butylethylene sulfide).

the symmetry of the space group $P3_121$ for the subcell. In order to improve molecular model I, the constrained least-squares method was applied using only the reflections from the subcell of the space group $P3_121$. The asymmetric unit in this case corresponds to one monomeric unit. The discrepancy factor R was 0.21 for 41 independent reflections. Next, the constrained least-squares method was applied to the original unit cell for the refinement of the actual crystal structure. Since the number of parameters to be refined was very large as compared with the number of observed reflections, the conformation of the main chain was fixed as the uniform (3/1) helix obtained from the refinement of the subcell. All hydrogen atoms were neglected. The parameters refined were a scale factor, an overall isotropic temperature factor, positions of molecular chains, and rotation angles of side groups, $C(CH_3)_3$. Figure 6a shows the crystal structure of the active species thus obtained. Figure 6b shows the upward and downward helices which occupy the same site. The fractional atomic coordinates are listed in Table V. Table VI gives the comparison between the observed and calculated spacings and intensities. An overall isotropic temperature factor was 13.0 Å^2. The discrepancy factor R was 0.20 for the independent 79 reflections.

An alternative crystal structure in which the axes of three molecular chains coincide with the three nonequivalent 3_1 axes in the unit cell was also examined. However, the final result was essentially the same as those shown in Figure 6.

Results and Discussion

Molecular Structure. The molecular structures of optically active and inactive species have the same main conformation: a right-handed (3/1) helix for the sinister chain and a left-handed one for the rectus chain. Figure 7 shows the molecular structure of inactive species. The internal rotation angles are listed in Table VII. The side chains are disposed in the staggered position in the inactive species; however, this is not always the case in the active species. According to the conformational analysis, the staggered disposition of the side chains in the isolated polymer chain is favorable. Therefore,

Table V
Atomic Parameters in Fractional Coordinates of Active Polymer[a]

	Up			Down		
	x	*y*	*z*	*x*	*y*	*z*
S(1)	0.383	−0.036	0.000	0.261	−0.003	0.138
C(1)	0.447	0.089	−0.006	0.314	0.121	0.141
C(2)	0.386	0.126	0.071	0.413	0.164	0.063
C(3)	0.440	0.231	0.063	0.458	0.269	0.069
C(4)	0.383	0.269	0.168	0.553	0.310	0.167
C(5)	0.531	0.267	0.178	0.467	0.306	−0.152
C(6)	0.458	0.263	−0.162	0.399	0.296	0.197
S(2)	0.351	0.088	0.334	0.413	0.127	−0.200
C(7)	0.226	0.028	0.328	0.484	0.074	−0.193
C(8)	0.189	−0.070	0.404	0.428	−0.026	−0.269
C(9)	0.084	−0.122	0.397	0.487	−0.071	−0.261
C(10)	0.045	−0.186	0.584	0.430	−0.170	−0.184
C(11)	0.050	−0.053	0.402	0.524	−0.071	−0.478
C(12)	0.051	−0.178	0.197	0.568	−0.017	−0.114
S(3)	0.227	−0.069	0.667	0.390	−0.027	−0.532
C(13)	0.287	−0.132	0.660	0.266	−0.098	−0.523
C(14)	0.385	−0.071	0.737	0.223	−0.042	−0.601
C(15)	0.437	−0.125	0.729	0.118	−0.102	−0.591
C(16)	0.536	−0.062	0.660	0.074	−0.053	−0.703
C(17)	0.437	−0.163	0.945	0.088	−0.194	−0.695
C(18)	0.389	−0.205	0.576	0.087	−0.118	−0.364

[a] Numbers of the atoms are the same as Table II.

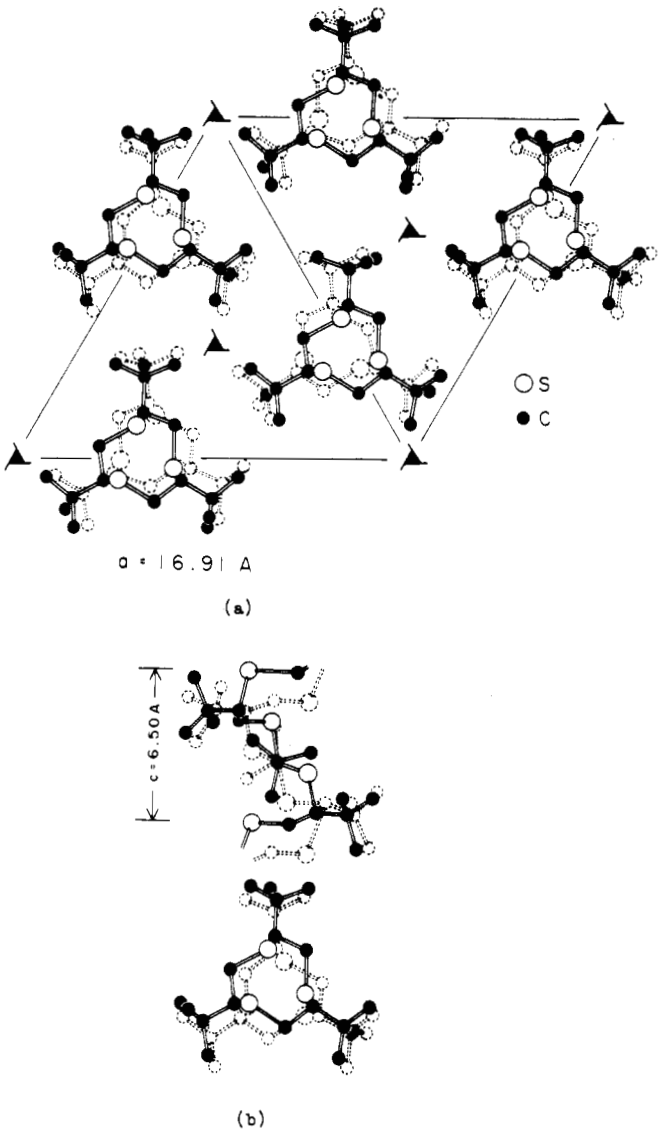

Figure 6. Crystal structure of optically active poly(*tert*-butylethylene sulfide). The upward chains are shown in solid lines and downward ones in broken lines. The lower figure shows the side view of upward and downward chains disposed at one site.

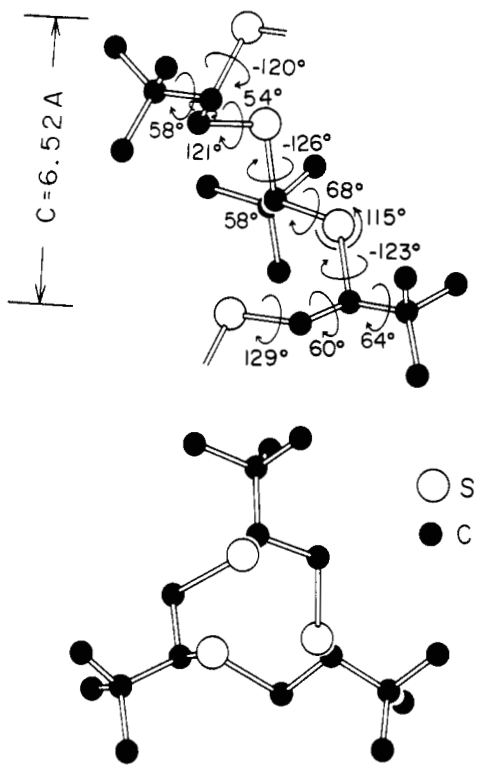

Figure 7. Molecular structure of optically inactive poly(*tert*-butylethylene sulfide).

the deviation from the staggered disposition of the side chains in the active species should be interpreted in terms of the intermolecular interactions.

Table VIII lists the conformations of several poly(alkylene oxides) and poly(alkylene sulfides). In the case of poly(*tert*-butylethylene sulfide), the internal rotation angles about the two neighboring C–S bonds are $\tau_1 = 122°$ (S) and $\tau_3 = -123°$ ($\bar{S}$) [cf. $\tau_1 = 180°$ and $\tau_3 = -97°$ for poly(*tert*-butylethylene oxide)]. Since the C–S bond length 1.82 Å is appreciably longer than the C–O bond length 1.43 Å, the conformation of S or $\bar{S}$ about the C–S bond both seem energetically feasible. If τ_1 and τ_3 are assumed to be, for simplicity, exactly 120 and −120°, respectively, then H(1), C(1), S(1), C(2), and H(2) atoms are all coplanar; the interatomic distances and van der Waals interaction energies (in parentheses, in kcal/mol) of this form are shown in Figure 8, in which the corresponding values for poly(*tert*-butylethylene oxide) are also shown. For the oxide, the conformation ($\tau_1 = 120°$ and $\tau_3 = -120°$) seems to be infeasible because of the repulsive steric interactions of C(2)···H(1) and H(1)···H(2) in addition to the high internal rotation barriers for skew form. For the sulfide, on the contrary, these pairs are no longer repulsive but are now attractive. Alternatively, when τ_2 is assumed to be 60° as in the actual poly(*tert*-butylethylene sulfide) chain, only the $\bar{S}$ conformation is feasible for τ_3, this is because the T, G, $\bar{G}$, and S conformations produce a high degree of steric hindrance between S, $C(2)H_2$, and CH_3 groups. Similarly with respect to τ_1, the conformations of S and T are feasible, but C(1) and C(3) atoms can come into close contact in S conformation. In poly(*tert*-butylethylene oxide) similar steric hindrance arises in the conformations of T, G, and $\bar{G}$ for τ_3. In the oxide, however, the conformation of $\bar{S}$ is infeasible as aforementioned, and then τ_3 is displaced from $\bar{S}$ toward $\bar{G}$, where the steric hindrance is less than that of T or G; the cooperative deviations of neighboring internal rotation angles of $\tau_2 = 73°$ and $\tau_3 = -97°$ from 60° or −60° can release the steric hindrance between $-C(2)H_2-$ group and O(0) atom. The existence of the S (122°) and $\bar{S}$ (−123°) conformations in poly(*tert*-butylethylene sulfide) was supported by the low value of the intramolecular potential energy calculated for the x-ray structure, 3.3 kcal/

Table VII
Comparison between the Conformations (deg) of Optically Active and Inactive Poly(*tert*-butylethylene sulfide)

	Inactive[a]	Active	
		Up	Down
τ_1[b]	122	122	
τ_2	61	60	
τ_3	−123	−123	
τ_4	64	68	13
	58	97	70
	58	22	20

[a] Values of τ_1, τ_2, and τ_3 are averaged ones. [b] τ_1, τ_2, τ_3, and τ_4 give the internal rotation angles, respectively, as shown below.

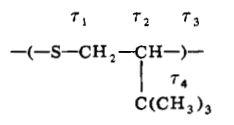

Table VIII
Molecular Conformations (deg) of Poly(alkylene sulfides) and Poly(alkylene oxides)

R	-(-S——CH_2——C*HR-)- τ_1	τ_2	τ_3		-(-O——CH_2——C*HR-)- τ_1	τ_2	τ_3	
H	60	180	60	Glide[13]	−176	68	−177	(7/2) helix[14]
					180	180	180	Planar zigzag[15]
CH_3	−160	180	160	(2/1) helix[3]	−165	180	165	(2/1) helix[16]
$CH(CH_3)_2$					180	67	−70	(2/1) helix[6]
$C(CH_3)_3$								
Inactive	122	61	−123	(3/1) helix	180	73	−97	(9/4) helix[2]
Active	122	60	−123	(3/1) helix				

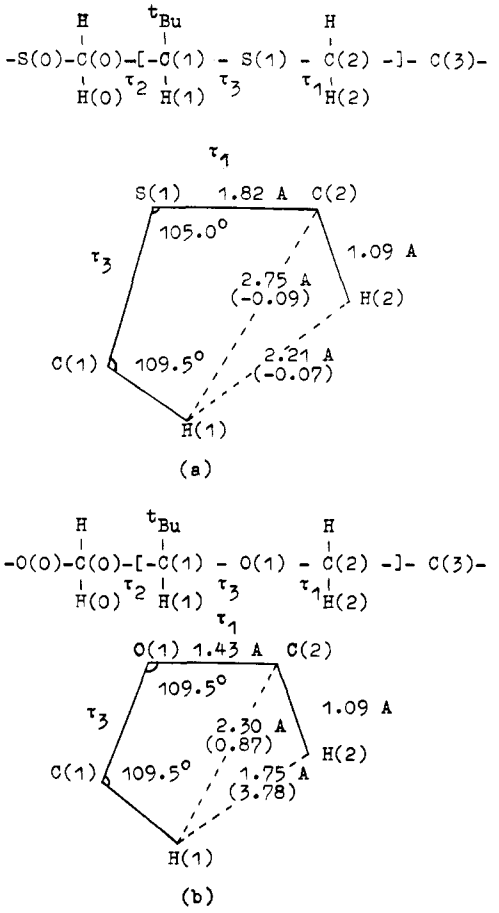

Figure 8. Interatomic distances and van der Waals interaction energies (in parentheses, in kcal/mol) for the conformation of τ_1 = 120° and τ_3 = −120°: (a) sulfide; (b) oxide.

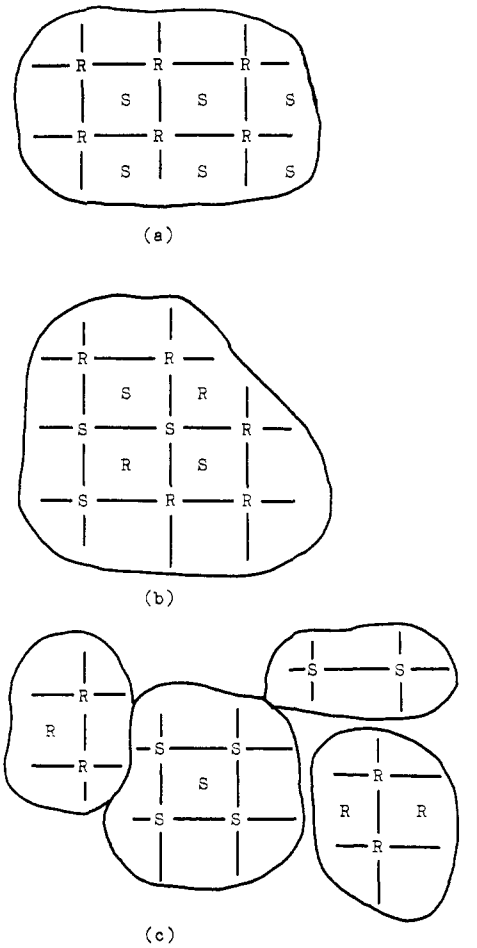

Figure 9. Ways of the optical compensation of optically inactive isotactic polymers: (a) compensation in a unit cell (racemic lattice); (b) compensation in a crystallite; (c) intercrystallite compensation. R and S denote rectus and sinister polymer chains, respectively.

mol of monomeric unit. In poly(*tert*-butylethylene oxide), the conformation of τ_3 = −97° was found to be the intramolecular potential minimum. Therefore, the values of τ_3 = −123° and τ_1 = 122° in poly(*tert*-butylethylene sulfide) as well as τ_3 = −97° in poly(*tert*-butylethylene oxide) are considered to be primarily due to the intramolecular interactions.

Crystal Structures and Optical Compensation. Figure 9 shows the possible kinds of optical compensation in optically inactive isotactic polymers, already proposed:[2,3] (a) compensation in the unit cell, i.e., a racemic lattice, (b) compensation in the crystallite, and (c) intercrystallite compensation. Table IX presents the modes of optical compensation found in several isotactic polymers whose crystal structures have been determined in this laboratory. All polymers except poly(*tert*-butylethylene sulfide) and poly(*tert*-butylethylene oxide) racemize as in the case of (c), in which the optical compensation is attained between antipode crystallites. Only one example has been found for case (a), form I of poly(*tert*-butylethylene oxide) in which the upward and downward chains occupy one site in the lattice with the same probability of 0.5 (statistically disordered structure). The unit cell of the optically inactive species of poly(*tert*-butylethylene sulfide) determined in the present study contains two pairs of rectus and sinister chains without any irregularity in the packing and the optical activity is compensated as in case (a).

Figure 10 shows schematically the crystal structures of optically active and inactive poly(*tert*-butylethylene sulfide). The mechanism of optical compensation in the unit cell for the inactive species is easily understood. The vertices of the triangles indicate the positions of the tertiary carbon atoms of the *tert*-butyl groups and added numerical values are their *z* coordinates. Although the crystals of the inactive species are monoclinic, differing from the trigonal structure of the active species, the monomeric units in the neighboring chains arranged along the *a* axis are mutually disposed with a height difference of about *c*/3.

Table IX
Optical Compensation of Several Polymers

$-(-S-CH_2-\overset{*}{C}H(C(CH_3)_3)-)-$	Racemic lattice	$-(-O-CH_2-\overset{*}{C}H(C(CH_3)_3)-)-$	Racemic lattice (form I)[2]; Intercrystallite (form II)
$-(-S-CH_2-\overset{*}{C}H(CH_3)-)-$	Intercrystallite[3]	$-(-O-CH_2-\overset{*}{C}H(CH(CH_3)_2)-)-$	Intercrystallite
$-(-O-C(=O)-CH_2-\overset{*}{C}H(CH_3)-)-$	Intercrystallite[4]	$-(-O-C(=O)-CH_2-\overset{*}{C}H(C_2H_5)-)-$	Intercrystallite[5]

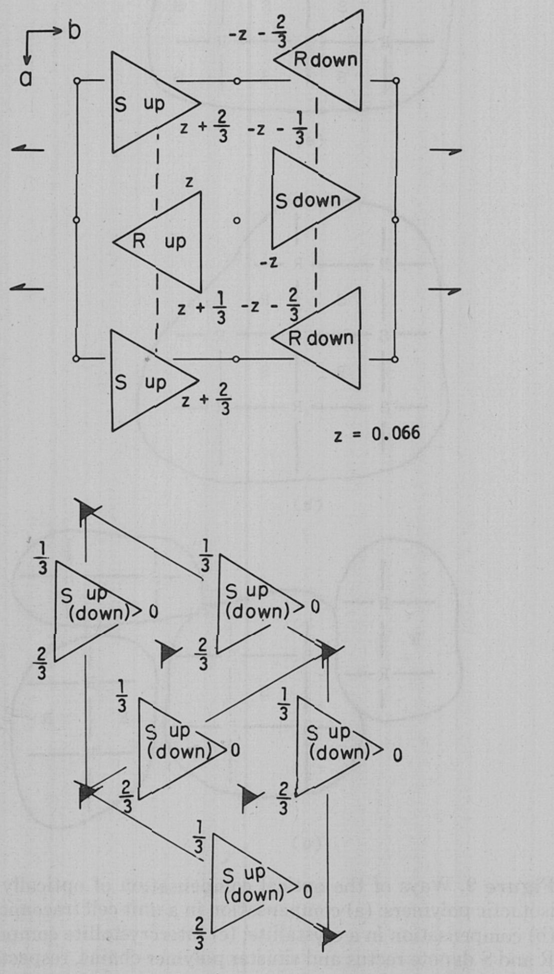

Figure 10. Schematic figures of crystal structures of optically inactive (top) and active poly(*tert*-butylethylene sulfide) (bottom). Numerical values show *z* coordinates of tertiary carbon atoms of *tert*-butyl group.

Variations of x-ray fiber photographs of the active species with annealing are characteristic as is shown in Figure 11. Only the reflections indexed by the aforementioned subcell appear before annealing (Figure 11a). The other reflections appear after annealing at 90 °C but they are broad (Figure 11b). They appear clearly as Bragg reflections after annealing at 145 °C, but they are still slightly broader than the reflections indexed by the subcell (Figure 11c). The annealing effect, therefore, may be interpreted as follows. Before annealing, upward and downward molecular chains are grossly packed as paracrystals represented approximately by the subcell. The annealing promotes the regularity of molecular packing, and the structure is explained by having a large unit cell which contains three molecular chains. Nevertheless, the larger temperature factor (13.0 Å^2) of the active species as compared to that of the inactive species (8.6 Å^2) seems to be indicative of the inherent disorder in the active species with respect to the arrangement of upward and downward molecular chains.

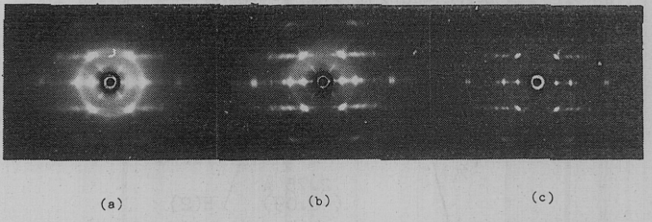

Figure 11. X-ray fiber photographs of the active species: (a) before annealing; (b) annealed at 90 °C for 40 h; (c) annealed at 145 °C for 20 h.

The difference between the crystal structures of the optically active and inactive species seems to greatly influence the following physical properties, although other factors such as crystallinity, crystallite perfection, etc., could not be ignored. (1) The melting point (210 °C) of the inactive species is about 50 °C higher than that (162 °C) of the active species. (2) The inactive species has rather limited solubility in benzene, whereas the active species dissolves in benzene readily.

Supplementary Material Available: Tables IV and VI containing observed and calculated spacings and structure factors for inactive and active poly(*tert*-butylethylene sulfide), respectively (6 pages). Ordering information can be found on any current masthead page.

References and Notes

(1) (a) Osaka University; (b) Université de Paris VI.
(2) H. Sakakihara, Y. Takahashi, H. Tadokoro, N. Oguni, and H. Tani, *Macromolecules*, **6**, 205 (1973).
(3) H. Sakakihara, Y. Takahashi, H. Tadokoro, P. Sigwalt, and N. Spassky, *Macromolecules*, **2**, 515 (1969).
(4) M. Yokouchi, Y. Chatani, H. Tadokoro, K. Teranishi, and H. Tani, *Polymer*, **14**, 267 (1973).
(5) M. Yokouchi, Y. Chatani, H. Tadokoro, and H. Tani, *Polym. J.*, **6**, 248 (1974).
(6) Y. Takahashi, H. Tadokoro, T. Hirano, A. Sato, and T. Tsuruta, *J. Polym. Sci., Polym. Phys. Ed.*, **13**, 285 (1975).
(7) R. S. Cahn, C. K. Ingold, and V. Prelog, *Experientia*, **12**, 81 (1960).
(8) P. Dumas, N. Spassky, and P. Sigwalt, *Makromol. Chem.*, **156**, 55 (1972).
(9) P. Dumas, N. Spassky, and P. Sigwalt, *J. Polym. Sci., Polym. Chem. Ed.*, **12**, 1001 (1974).
(10) T. Miyazawa, *J. Polym. Sci.*, **55**, 215 (1961).
(11) K. Tai and H. Tadokoro, *Macromolecules*, **7**, 507 (1974).
(12) S. Arnott and A. J. Wonacott, *Polymer*, **7**, 157 (1966).
(13) Y. Takahashi, T. Sato, H. Tadokoro, and Y. Tanaka, *J. Polym. Sci., Polym. Phys. Ed.*, **11**, 233 (1973).
(14) Y. Takahashi, H. Tadokoro, and Y. Chatani, *J. Macromol. Sci., Phys.*, **2**, 361 (1968).
(15) Y. Takahashi and H. Tadokoro, *Macromolecules*, **6**, 672 (1973).
(16) Y. Takahashi, I. Sumita, and H. Tadokoro, *J. Polym. Sci., Polym. Phys. Ed.*, **11**, 2113 (1973).
(17) M. Cesari, G. Perego, and W. Marconi, *Makromol. Chem.*, **94**, 194 (1966).